Numerical Study of Nonlinear Spectral Analysis for Measuring the Recovery Time of Saturable Absorbers

Bowen Liu*
Research Center for Advanced Science and Technology
The University of Tokyo
Tokyo, Japan
bwliu@cntp.t.u-tokyo.ac.jp

Maolin Dai
Research Center for Advanced Science and Technology
The University of Tokyo
Tokyo, Japan
syama@cntp.t.u-tokyo.ac.jp

Takuma Shirahata
Research Center for Advanced Science and Technology
The University of Tokyo
Tokyo, Japan
set@cntp.t.u-tokyo.ac.jp

Shinji Yamashita
Research Center for Advanced Science and Technology
The University of Tokyo
Tokyo, Japan
syama@cntp.t.u-tokyo.ac.jp

Sze Yun Set
Research Center for Advanced Science and Technology
The University of Tokyo
Tokyo, Japan
set@cntp.t.u-tokyo.ac.jp

***Abstract*—Numerical exploration of nonlinear spectral analysis for measuring saturable absorption recovery time demonstrates monotonic relationship between it and difference spectra. The results also reveal a certain tolerance to self-phase modulation effects, allowing all-fiber system configurations.**

Keywords—Nonlinear spectral analysis, saturable absorption, recovery time, self-phase modulation

I. INTRODUCTION

Ultrafast fiber lasers have been attracting intensive attention in practical applications such as telecommunications, micromachining, laser marking and spectroscopy, as well as in cutting-edge research fields of nonlinear optics. To step into the sub-picosecond time domain, passive mode-locking could be an ideal choice among the few options, which depends on a saturable absorber (SA) to initialize and narrow intra-cavity pulses. No matter a real SA made from materials that the ground state becomes depleted at high optical intensity, or an artificial SA based on nonlinear effects, either of them provides nonlinear saturable absorption (NSA) [1]. This will reduce the loss until saturation as light intensity increases, although artificial SAs like Kerr lensing do not absorb any light actually. Particularly, SAs that exploiting real media is conducive to self-starting mode-locking due to the generally longer recovery times [2]. Whereas slow response is not always desired especially for ultra-short pulse generation. How fast or slow a SA is relative to the transmitted pulse duration. Selecting a SA with appropriate recovery time can improve the performance of emitted pulses and enhance the stability [3]. Basically different materials have different recovery times, however even the same material can exhibit differences in recovery times if processed differently, as shown in table 1.

Pump-probe spectroscopy is one of the most accurate approaches to measure the NSA of a SA, in which the sample is firstly hit by high peak-power pump pulses and then hit again by a relatively weaker probe pulse to catch the excitation information after an adjustable time delay. Thus, the characteristics of a SA is measured and reflected via the relationship between probe signal and time delay [14]. However, this free-space light path based method usually suffers from high system complexity and poor signal-to-noise ratio (SNR). The setup for pump-probe measurement can be complicated and sometimes require specialized equipment since the system is sensitive to the alignment and any misalignment can lead to severe errors in the results. A low SNR is also caused as the probe signal is typically very small compared to the pump pulses. In addition, asynchrony can badly affect the accuracy of results as some of the pump-probe measurements rely on two ultra-short pulse sources to provide pump and probe signals simultaneously [15]. These lasers are required to be strictly synchronized to ultra-low relative timing jitter, which further adds complexity and challenges to the system. These drawbacks make it full of charm to explore an easy-to-use and fiber light path based alternative solution.

In this paper, we proposed a novel all-fiber method of nonlinear spectral analysis to measure the characteristics of a SA. The numerical study is performed to tap in-depth insights into nonlinear saturable absorption. Characteristics peaks in the difference spectra are demonstrated. A monotonic increasing correlation is revealed between the recovery time of a SA and the characteristic peaks. Meanwhile, the impacts of self-phase modulation effects are investigated to evaluate the ability of this all-fiber measurement system to perform accurate measurements. The results could help enrich understanding to ultrafast process of nonlinear saturable absorption, exploring potential solutions for charactering SAs.

TABLE I. RECOVERY TIMES OF COMMON SA MATERIALS

Materials	*Recovery time*	*Reference*
Bi_2Te_3	0.5 ps	[4]
BP	2.4 ps	[5]
BPQD	82~102 ps	[6]
CNT	1 ps	[7]
Graphene	1.15~1.39 ps	[8]
MoS_2	1.2~2.4, 90~110 ps	[9,10]
$MoSe_2$	220 ps	[11]
SESAM	0.5 ps	[12]
WS_2	1.3, 100 ps	[13]

II. Principle and Setup

The schematic diagram of the simulation setup is illustrated in Fig. 1, consisting of a simulating femtosecond pulsed laser and the system to conduct nonlinear spectral analysis. The pulses are generated from random quantum noise in gain fiber. Their propagation and dynamic behaviors in fibers are governed by the Nonlinear Schrödinger Equation (NLE) [16], in which the gain g with a parabolic profile, the loss α, the group velocity dispersion β_2 and its slope β_3 and self-phase modulation γ are taken into account.

$$\frac{\partial A}{\partial z}+\frac{i}{2}\left(\beta_2+igT_2^2\right)\frac{\partial^2 A}{\partial t^2}-\frac{1}{6}\beta_3\frac{\partial^3 A}{\partial t^3}=i\gamma|A|^2A+\frac{1}{2}(g-\alpha)A \quad (1)$$

The numerical solution of NLE could be calculated by Split Step Fourier Method (SSFM), and the parameters can be found in our previous works [17].

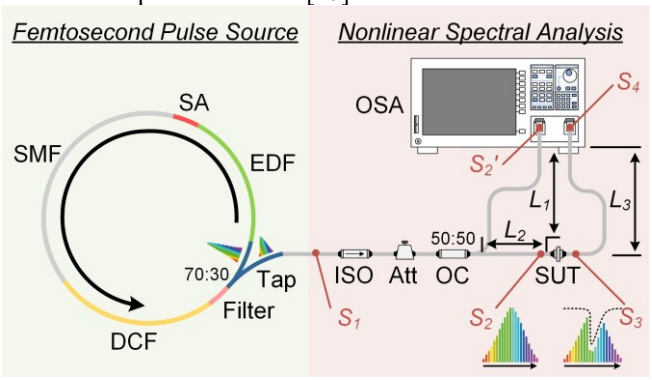

Fig. 1. Schematic diagram of the simulation setup that consists of a femtosecond pulse source and an nonlinear spectral analysis system. Att: Attenuator, DCF: Dispersion Compensating Fiber, EDF: Erbium-Doped Fiber, ISO: Isolator, OC: Optical Coupler, OSA: Optical Spectral Analyzer, SA: Saturable Absorber, SMF: Single Mode Fiber, SUT: Sample Under Test.

In nonlinear spectral analysis system, the pulse states at four positions are monitored (S_1 to S_4). The total length of pigtail fiber between S_1 (laser output port) to S_2 (SA input port) is the same to the one between S_1 to S_2' (OSA input port for reference light), set as 100 cm. The pigtail fiber from S_3 (SA output port) to S_4 (OSA input port for detection light) is 40-cm long (L_3). Thus, the nonlinear saturable absorption characteristics are analyzed through the difference spectra of S_4 versus S_2' (S_2). The pulse traces and optical spectra of S_1 to S_4 are shown in Fig. 2(a) and 2(b). The pulse duration is around 555 fs in a sech^2 profile, and its energy is 133.16 pJ. Due to the dispersion and nonlinear effects in the fibers, the pulse shape undergoes some degree of distortion during propagation, as well as changes in phase. While characteristics of SAs still could be detected via this nonlinear spectral analysis method. The difference pulse trace and optical spectrum when the recovery time is 10 ps are depicted in Fig. 2(c) and 2(d). In the zoom-in inset of figure 2(d), two characteristic peaks are found. The interval of these characteristic peaks $\Delta\lambda$ is measured to summarize the correlation with saturable absorption recovery time. Figure 2(e) presents the normalized saturable absorption losses with a variable recovery time from 0.1 ps to 30 ps, from fast to slow SAs. The nonlinear loss q of a SA is described by Eq. (2), in which the modulation depth q_0, the recovery time τ and the saturation fluence E_{sat} play significant roles.

$$\frac{dq}{dt}=-\frac{q-q_0}{\tau}-\frac{q|A(t)|^2}{E_{sat}} \quad (2)$$

Here, the NSA losses are normalized to q_0 and the pulses are adjusted to fully yet not over saturated. Therefore, the results mainly depends on the recovery time. The highest resolution of simulation is 25 fs in the time domain, and 0.02 nm in the frequency domain—the same as most of commercial OSA.

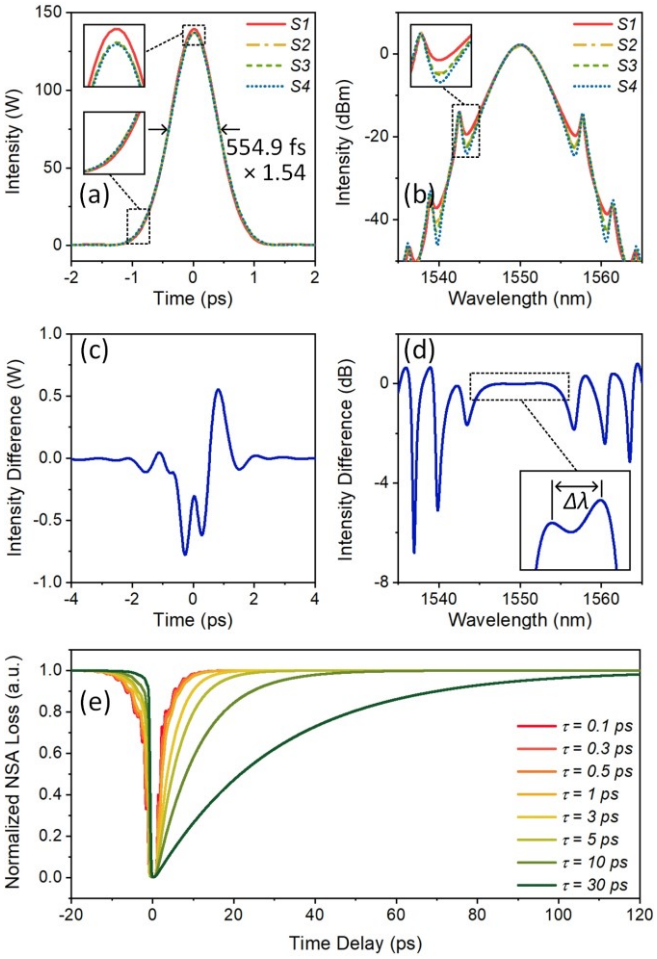

Fig. 2. (a) Pulse profiles and (b) optical spectra of S1 to S4, (c) difference pulse profile and (d) difference optical spectrum of S4 versus S2, (e) normalized nonlinear saturable absorption loss of samples with varied recovery time from 0.1 ps to 30 ps.

III. Results and Discussion

The results of difference spectra with different recovery times are shown in Fig. 3(a). With recovery time growing from 0.1 ps to 30 ps, the intervals of characteristic peaks in optical spectrum increase synchronously. In addition, the asymmetry of the spectral envelope of the long-wave and short-wave parts becomes more and more serious. The recovery time reflects the time delay for the absorption loss of a SA to recover when the trailing edge of pulse pass through it—this will introduce asymmetric absorption loss at the leading and trailing edges of the pulse. This trend is concluded as shown in Fig. 3(b). The characteristic peaks interval exhibits a monotonic increasing relationship versus recovery time, regardless of a slight rebound in fast absorption regime. The one-phase exponential decay function (ExpDec1) fits the simulation results very well, indicating the maximum variable range of $\Delta\lambda$ is 2.63 nm, from 2.97 nm to 5.60 nm of ultrafast to extremely slow SAs. Meanwhile, as the recovery time increases, the relative walk-off of characteristic peaks become smaller.

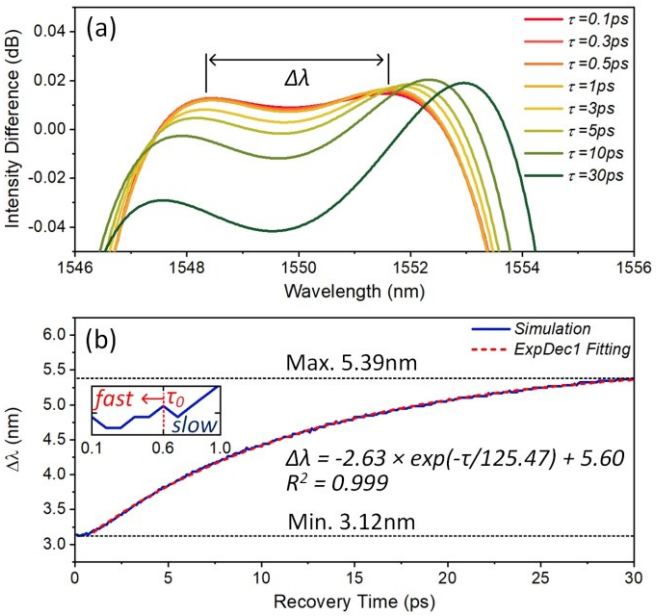

Fig. 3. (a) Difference spectra of S4 versus S2 with varied recovery time from 0.1 ps to 30 ps, (b) the specrtal interval of charactrstic peaks Δλ increases as the recovery time τ grows, showing an exponential positive correlation.

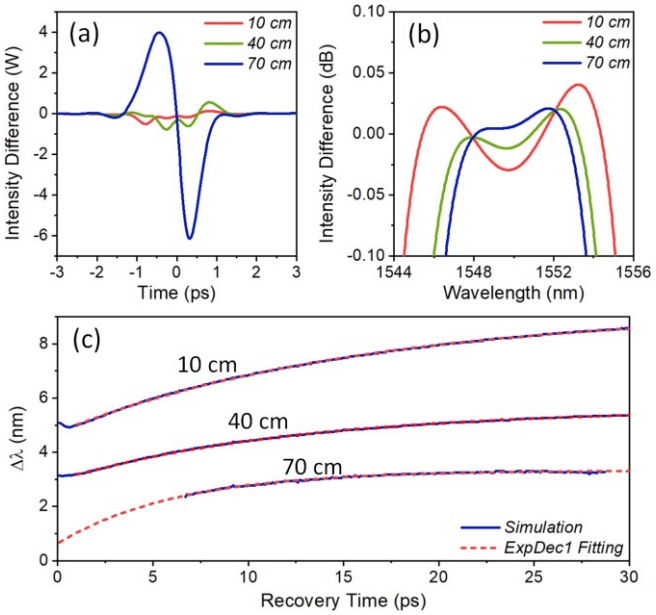

Fig. 4. (a) Difference pulse profiles and (b) difference optical spectra of S4 versus S2 when the lenths of pigtail fiber between S3 and S4 are 10 cm, 40 cm and 70 cm, (c) the relationships between the specrtal interval of charactrstic peaks Δλ and the recovery time τ with a 10-cm, 40-cm or 70-cm long pigtail fiber.

Furthermore, given that the SPM effect excited by the high peak power pulse in standard optical fibers will impose distortion to the pulse shape when actually measuring the saturable absorption characteristics, the impacts of the pigtail fiber inserted between S_3 and S_4 on the simulation results is investigated. The length L_3 is changed from 10 cm to 70 cm. The difference pulse traces and optical spectra are illustrated in Fig. 4(a) and 4(b), where the adverse impacts of SPM effects become much more serious as longer fiber being used. For 10-cm case, the hump of characteristic peaks are greatly stronger, which means a higher sensitivity to recovery time changes compared with 40-cm and 70-cm ones. In addition, the relationships between Δλ and recovery time are summarized in Fig. 4(c). Except for 70-cm simulation results, which are incomplete due to severe impacts of SPM effects induced unmeasurable data, the other cases conform to the monotonically increasing trends, and the shorter the fiber length, the greater the slope of the simulation results change.

IV. Conclusion

To conclude, we report the numerical study of nonlinear spectral analysis for measuring saturable absorption recovery time. The difference spectra between input and output of saturable absorbers are analyzed, where the interval of characteristic peaks is demonstrated to be monotonically increasingly correlated to recovery time. Moreover, the impacts of SPM effects are investigated. A certain tolerance is allowed by nonlinear spectral analysis, although the SA characteristics would be severe degraded under strong SPM effects, which indicates potential all-fiber configurations. The shorter the pigtail inserted, the higher the sensitivity of the characteristic peak response recovery time. The results reveal a prospective approach to measure saturable absorption characteristics by a low-complexity and easy-to-use system, and tap into deep insights of nonlinear saturable absorption.

Acknowledgment

This work is supported by China Scholarships Council (No.202006160019) and the Japan Society for the Promotion of Science (JSPS) Grant-in-Aid for Scientific Research (S) 18H05238 and (A) 22H00209.

References

[1] S. Y. Set, H. Yaguchi, Y. Tanaka, and M. Jablonski, "Laser mode locking using a saturable absorber incorporating carbon nanotubes," J. Light. Technol., vol. 22, pp. 51-56, January 2004.

[2] E. P. Ippen, L. Y. Liu, and H. A. Haus, "Self-starting condition for additive-pulse mode-locked lasers," Opt. Lett., vol. 15, pp. 183-185, February 1990.

[3] C. Ma, W. Huang, Y. Wang, J. Adams, Z. Wang, J. Liu, Y. Song, Y. Ge, Z. Guo, L. Hu, and H. Zhang, "MXene saturable absorber enabled hybrid mode-locking technology: a new routine of advancing femtosecond fiber lasers performance," Nanophotonics, vol. 9, pp. 2451-2458, April 2020.

[4] A. Q. Wu, X. Xu, and R. Venkatasubramanian, "Ultrafast dynamics of photoexcited coherent phonon in Bi_2Te_3 thin film," Appl. Phys. Lett., vol. 92, 011108, January 2008..

[5] Y. Wang, G. Huang, H. Mu, S. Lin, J. Chen, S. Xiao, Q. Bao, and J. He, "Ultrafast recovery time and broadband saturable absorption properties of black phosphorus suspension," Appl. Phys. Lett., vol. 107, 091905, August 2015.

[6] R. Chen, X. Zheng, and T. Jiang, "Broadband ultrafast nonlinear absorption and ultra-long exciton relaxation time of black phosphorus quantum dots," Opt. Express, vol. 25, pp. 7507-7519, April 2017.

[7] T. R. Schibli, K. Minoshima, H. Kataura, E. Itoga, N. Minami, S. Kazaoui, K. Miyashita, M. Tokumoto, and Y. Sakakibara, "Ultrashort pulse-generation by saturable absorber mirrors based on polymer-embedded carbon nanotubes," Opt. Express, vol. 13, pp. 8025-8031, October 2005.

[8] A. E. Nikolaenko, N. Papasimakis, E. Atmatzakis, Z. Luo, Z. Shen, F. D. Angelis, S. A. Boden, E. D. Fabrizio, and N. I. Zheludev, "Nonlinear graphene metamaterial," Appl. Phys. Lett., vol. 100, 181109, April 2012.

[9] Q. Wang, S. Ge, X. Li, J. Qiu, Y. Ji, J. Feng, and D. Sun, "Valley carrier dynamics in monolayer molybdenum disulfide from helicity-resolved ultrafast pump-probe spectroscopy," ACS Nano, vol. 7, pp. 11087-11093, November 2013.

[10] R. Wang, B. A. Ruzicka, N. Kumar, M. Z. Bellus, H.-Y. Chiu, and H. Zhao, "Ultrafast and spatially resolved studies of charge carriers in atomically thin molybdenum disulfide," Phys. Rev. B, vol. 86, 045406, July 2012.

[11] G. Wang, G. Liang, A. A. Baker-Murray, K. Wang, J. Wang, X. Zhang, D. Bennett, J. Luo, J. Wang, P. Fan, and W. J. Blau, "Nonlinear optical performance of few-layer molybdenum diselenide as a slow-saturable absorber," Photon. Res., vol. 8, no. 7, pp. 674-680, July 2018.

[12] Y. G. Wang, X. Y. Ma, C. Y. Li, Z. G. Zhang, B. Y. Zhang, and Z. G. Zhang, "A passively mode-locked diode-end-pumped Nd:YAG laser with a semiconductor saturable absorber mirror grown by metal organic chemical vapor deposition," Chin. Phys. Lett., vol. 20, pp. 1960-1962, November 2003.

[13] V. Vega-Mayoral, D. Vella, T. Borzda, M. Prijatelj, I. Tempra, E. A. A. Pogna, S. D. Conte, P. Topolovsek, N. Vujicic, G. Cerullo, D. Mihailovic, and C. Gadermaier, "Exciton and charge carrier dynamics in few-layer WS_2," Nanoscale, vol. 8, pp. 5428-5434, March 2016.

[14] M. Maiuri, M. Garavelli, and G. Cerullo, "Ultrafast Spectroscopy: State of the Art and Open Challenges," J. Am. Chem. Soc., vol. 142, pp. 3-15, December 2019.

[15] Y. Hayasaki, S. Fukuda, S. Hasegawa, and S. Juodkazis, "Two-color pump-probe interferometry of ultra-fast light-matter interaction," Sci. Rep., vol. 7, 10405, September 2017.

[16] J. Lee, S. Kwon, L. Zhao, and J. H. Lee, "Investigation into the impact of the recovery time of a saturable absorber for stable dissipative soliton generation in Yb-doped fiber lasers," Optics Exp., vol. 29, pp. 21978-21991, July 2021.

[17] B. Liu, S. Yamashita and S. Y. Set, "Numerical analysis on the effects of spectral ripple for saturable absorber based mode-locking," Pacific-Rim Conference of Lasers and Electro-Optics (CLEO-PR) at Sapporo Japan, CTuA1B-02, July 2022., in press.